Craze Morphology and Molecular Orientation in the Slow Crack Growth Failure of Polyethylene

JOSÉ M. LAGARÓN,[1] GIANCARLO CAPACCIO,[2] LES J. ROSE,[2] BERT J. KIP[1]

[1] DSM Research, P.O. Box 18, 6160 MD Geleen, The Netherlands

[2] BP Chemicals, Applied Technology, P.O. Box 21, Grangemouth, Stirlingshire FK3 9XH, United Kingdom

Received 12 November 1998; accepted 4 September 1999

ABSTRACT: An optical microscopy study and a micro-Raman spectroscopy study were carried out on polyethylene samples subjected to an environmental stress crack resistance (ESCR) test. The aim was to elucidate the molecular deformation mechanisms associated with the failure process. It has been shown that in the early stages of the ESCR test, in a regime of low local stress, failure in the craze occurs via a brittle process with limited ductility and with molecular orientation being detected. As the experiment progresses, however, extensive fibrillation takes place. The molecular orientation in these fibrils was found to be comparable to that measured in cold-drawn samples. Moreover, the fibril molecular orientation decreased from the crack to craze tip and was found to be higher in the midrib part of the fibril (fibril failure point). As a consequence, fibril creep is the most likely mechanism of failure in the craze. Microscopy and Raman measurements showed that the extent of the brittle process is molecular weight-dependent, that is, the brittle process seems to operate longer at higher molecular weights. These observations are in agreement with a previous work which showed that the molecular stress per macroscopic strain/stress decreases with increasing molecular weight, therefore holding the high molecular weight craze in a regime of low local stress for longer testing times. Fibrils spanning the craze are envisaged as the anchor points that hold the structure during the process of failure. J Appl Polym Sci 77: 283–296, 2000

Key words: environmental stress crack resistance (ESCR)**;** polyethylene; micro-Raman spectroscopy; molecular orientation

INTRODUCTION

Slow crack growth is an important failure mechanism in polyethylene (PE). It takes place under the effect of an applied stress and can be accelerated by the presence of surfactants. In the latter case, the phenomenon is commonly referred to as environmental stress cracking (ESC). Over the past decade, this phenomenon was studied extensively by Brown and coworkers[1–9] and by Barry and Delatycki.[10,11] Notched samples under static tensile stress and in three-point bending showed a damage zone at the notch tip, which is made of highly voided material with a fibrillar structure. Several processes are thought to determine crack initiation and growth: Yield, yield propagation, and drawing are associated with the conversion of isotropic material into highly oriented fibrils. Fibrils, in turn, will undergo creep deformation and eventually rupture. The phenomenology of the process has received much attention over the years.[1–11] Also, Brown et al.[12] suggested that slow crack growth is controlled by the macroscopic creep behavior of the material. The role played by

Correspondence to: B. J. Kip.

Journal of Applied Polymer Science, Vol. 77, 283–296 (2000)

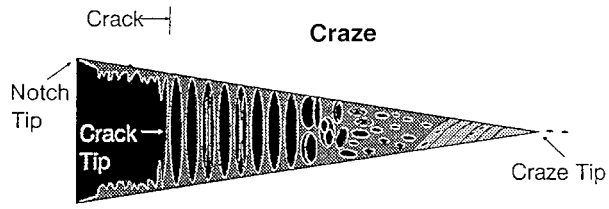

Figure 1 Sketch illustrating the used crack and craze terminology.

tie molecules and the relevance of their concentration were emphasized by Lustiger and Corneliusen.[13] These authors also discussed failure processes, which may take place in the interlamellar region of the material.

However, it was only recently that the gap between phenomenology and structure was bridged with the work by Rose et al.[14] These authors proposed a model in which the time-to-failure in slow crack growth is controlled by the creep behavior of the craze fibrils. They found a remarkably good correlation between ESC performance and a parameter related to the creep rate measured on samples drawn to their "natural draw ratio" (NDR). Figure 1 shows a sketch of the typical crack and craze morphology. A key assumption in the model is that the craze fibrils have, at failure, the same structure and orientation of a tensile-drawn specimen. While the experimental validation of the model supports this assumption, a detailed characterization of the craze fibrils was missing in PE. As opposed to the PE case, the characterization of the craze fibrils was extensive in glassy polymers.[15] In glassy polymers, it is found that the average draw ratio (deduced from SAXS, TEM, and optical interference data) of the craze fibrils is generally kept constant from the crack to craze tip. The average draw ratio significantly increases, though, at the craze tip. These observations suggest to the authors a "surface drawing" mechanism of failure rather than a "fibril creep" mechanism. The surface drawing model implies that the craze thickens by drawing new polymer from the craze interfaces into the craze fibrils, therefore maintaining the average extension ratio constant for a given surface area. The fibrils eventually fail by chain scission and entanglement loss during the drawing process. This is further substantiated by fibril breakdown being observed at the craze–bulk interface rather than at the midrib part, which, in turn, would suggest fibril creep as the failure mode. However, a good understanding of the molecular factors controlling crazing in glassy polymers cannot easily be applied to slow crack growth in PE[14,16] This refers to the fact that crazing in PE occurs well above the glass transition temperature (T_g), while in glassy polymers, it is confined to temperatures below the T_g. Also, differences in craze geometry (fibril size is much higher for PE) and in the slope of the plot "stress intensity" factor (K_c) versus "crack speed" were measured between glassy polymers and PE.

Micro-Raman spectroscopy has become a very powerful tool in molecular characterization. In particular, the high lateral and depth spatial resolution makes the technique a valuable tool for polymer characterization thanks to the development of the Confocal and Raman imaging systems.[17–19] The applications of this Raman technique in the polymer field to characterize the chemical nature, its structure (configuration and conformation), orientation, and morphology (i.e., amorphous or crystalline phase) is reaching a solid position among the analytical techniques. Over the past two decades, Raman spectroscopy has been widely used to characterize PE and the assignments of the main Raman bands are well known. The internal normal modes between 1000 and 1600 cm^{-1} are frequently used to study morphological structure (e.g., crystallinity, orientation, and molecular stress) and can be divided into three vibrational areas[20,21]:

1. C—C stretching between 1000 and 1200 cm^{-1}, sensitive to molecular orientation, stress, and conformation.
2. —CH_2— twisting vibrations around 1295 cm^{-1}, which can be used as an internal standard.
3. —CH_2— bending modes between 1400 and 1470 cm^{-1}, sensitive to chain packing (the 1415 cm^{-1} band is assigned to orthorhombic crystallinity).

A qualitative method for determining the molecular orientation, using the ratio of the 1130/1060-cm^{-1} Raman bands, was published.[22] These bands have different vibrational symmetries ($B_{3g} + B_{2g}$ and $A_g + B_{1g}$ for the 1060- and 1130-cm^{-1} bands, respectively).[22,23] Under certain polarization conditions, the A_g symmetry is active and the other $B_{1g} + B_{2g}$ symmetry is inactive, and in this geometry, if the molecules are oriented in the preferred direction, then the 1130-cm^{-1} band becomes stronger with respect to the 1060-cm^{-1} band. In addition to the molecular orientation,

Table I Some Material Properties and ESCR Notch Test Results of the Three Samples Studied

Sample	Density (kg/m^3)	M_w ($\times 10^3$) (g mol^{-1})	M_w/M_n	δSCB/1000C	NDR	ESCR (h) at 348 K	PE Type
HPE1	960	134	7.4	0	10.4	5	Homopolymer
HPE2	954	385	8.0	0	7	72	Homopolymer
CPE1	958	200	18.2	0.3(E)	8.7	10	Unimodal copolymer

δ, Short-chain branches (SCB); (E), ethyl branches.

the Raman spectra of PE also deliver information about molecular stress. In numerous studies,[24–26] it was shown that Raman band shifts are a result of molecular stress. This is believed to be a result of distortion of bond angles and bond lengths. Furthermore, a recent work[27] suggested that the transfer of stress at the molecular level is molecular structure-dependent and lower for higher molecular weights and copolymers.

In the work to be discussed here, Raman spectroscopy and microscopy were used for a detailed characterization of the structure of PE crazes. In particular, molecular orientation was measured at different positions in the craze and at different times under stress and compared with the orientation measured in cold-drawn samples.

EXPERIMENTAL

Materials and Sample Preparation

Two homopolymers and one copolymer were used in this study. Sample characteristics are summarized in Table I. This analysis was based on both optical microscopy observations and micro-Raman spectroscopy tests performed at different times during the environmental stress crack resistance (ESCR) experiment. A duplicate set of samples was removed after 0, 2, 4, 6, 8, and 9.9 h in the case of CPE1 and after 60% of the failure time for HPE1 and HPE2.

Sheets of 500-μm thickness were pressed between aluminum foils from pellet material in four steps: 5 min at 20 kN at 463 K, 5 min at 200 kN at 463 K, $<$200 kN cooling down to 308 K, and without pressure down to room temperature. From these sheets, dumbbell samples were die-stamped with a gauge length of 20 $\pm$ 0.5 mm and a width of 4 $\pm$ 0.1 mm (Model ISO 527-2:1993 type 5A). The dumbbells were conditioned in boiling water for 30 min to remove any residual stresses built up in the sample preparation procedure. The cold-drawing process was carried out on a Zwick 1455 stretching device with a constant rate of 10 mm/min until the full gauge length of the dumbbell was necked. The NDR is defined by this situation and was measured with an optical extensometer. The creep test was applied as a subsequent step of cold-drawing using a constant load obtained by reading-out the last stress held in the cold-drawing process. The creep test was applied for 180 min.

ESCR Test Conditions

A standard tensile ESCR test was performed by applying a constant stress at 348 K in a detergent solution on a notched sample (see sample shape in Fig. 2). The key feature of this test is that the notch crack develops under growing internal stress conditions at 348 K. The test terminates once the crack travels the full width and depth of the sample. The reader is referred to Figure 2 for a description of the ESCR test conditions and to Figure 1 for a description of the terminology used throughout the article.

Optical Microscopy

To measure crack length (crack + craze) displacement during the test, a TV camera setup with a calibrated TV screen placed onto the Olympus BX40 microscope was used and the objectives used were MLP5$\times$, MLP10$\times$, and MLP20$\times$ belonging to the MPLAN(F.N. 22) series. A microphotographic report was developed by the Axiophot setup (photographic camera and microscope) from Zeiss using reflected light and using different contrast methods such as darkfield, brightfield, and differential interference contrast (DIC).

Micro-Raman Spectroscopy

Micro-Raman spectroscopy was used to determine the molecular orientation in the crack and craze.

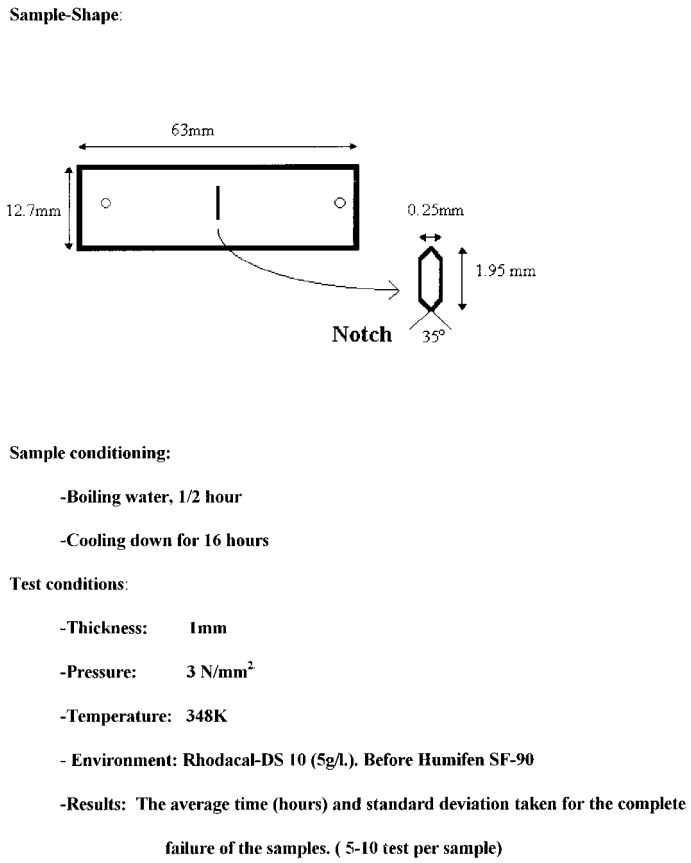

Figure 2 ESCR sample shape, sample conditioning, and test conditions.

A Jobin-Yvon U1000 spectrometer was used, fitted with 1800 or 600 grooves/mm gratings, employing 514-nm excitation, 25 mW at the sample, and a 1024-pixel diode array. A pinhole (300-μm diameter) was placed in the back focal plane of the microscope to improve the spatial resolution (confocal arrangement, lateral resolution ca. 1μm, depth resolution, fwhm, ca. 3 -μm). A microscope with a 50$\times$ short working distance objective was interfaced. A further description of the latter setup can be found in ref. 17. The LabRam system of Dilor with 1800 gratings, 100$\times$ objective, 632 nm excitation, 16 mW at the sample, 100-μm pinhole, and CCD detector was also used in some cases. The latter equipment provides an enhanced spatial resolution, that is, lateral resolution of <1 μm and a depth resolution of <2 μm.

The curve fitting of the recorded Raman spectra was performed using the fitting routine in the Grams Research 2000 software package (Galactic Industries). Voigt line shapes (convolution of Lorentzian and Gaussian band shapes) and linear baselines were used. Results of fitting typically look as shown in Figure 3. In the case of spectra recorded with the J-Y spectrometer equipped with 1800-g/mm gratings, the 1130 cm^{-1} had to be fitted with two bands to account for the asymmetric left-hand side of the band. The 1060-cm^{-1} band also had to be fitted with two components. In the case of spectra recorded with J-Y 600-g/mm gratings, the 1060 cm^{-1} was well fitted with only one band.

RESULTS AND DISCUSSION

Characterization of Samples by Optical Microscopy

By using the calibrated TV screen, the length of the cracks (crack + craze) was measured as a function of time for sample CPE1. From these measurements, a plot can be constructed of crack linear displacement (CLD) versus time [see Fig. 4(a)]. Figure 4(b) shows the plot in which the natural logarithm of the CLD is plotted versus time. For times in excess of 4 h, ln CLD exhibits a

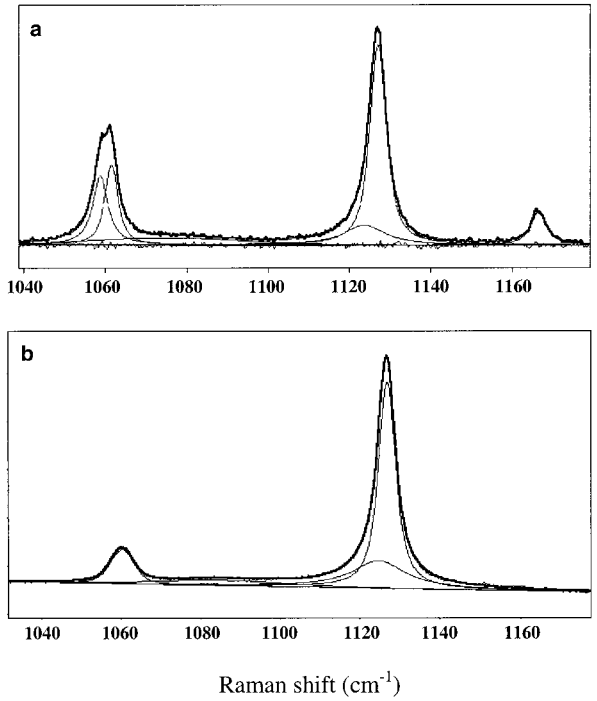

Figure 3 Curve-fitting of Raman spectra taken in sample CPE1 after the failure time in the ESCR test: (a) in undeformed (isotropic) material; (b) in highly oriented fibrils. The spectra were recorded with the J-Y Raman system equipped with 1800-g/mm gratings.

linear dependence upon time. This implies an experimental function of the following form:

$$\mathrm{CLD} = 1.43e^{0.43t} \qquad (1)$$

where the CLD is expressed as relative displacement in percent.

On the other hand, from 0 to 4 h, the sample does not seem to follow eq. (1) [see continuous line in Fig. 4(b)]. From the latter figure, two regimens are suggested during crack opening, which will be further evidence in the forthcoming discussion.

Observation by a microscope of the same sample at different times showed (results not shown) (i) a sharp craze tip at early hours and (ii) stress-whitening at the craze tip at long times [see Fig. 5(b)], as well as fibrils spanning the craze and having a larger size after 6 h (0.6 of the time to failure). These fibers are generally absent before 2 h. Furthermore, voids and failed fibrils are observed.

Samples HPE1 and HPE2 with relatively poorer and superior performance were also examined (see Fig. 5). When the ESCR test was interrupted after 0.6 of the time to failure, large differences were observed along the crack: Sample HPE1 shows a large crack opening with extensive fibril formation and a blunt craze tip, as illustrated in Figure 5(a,b). In contrast, for HPE2, a small crack opening, a sharp craze tip, and fewer fibrils are observed [Fig. 5c,d)]. Finally, from Fig-

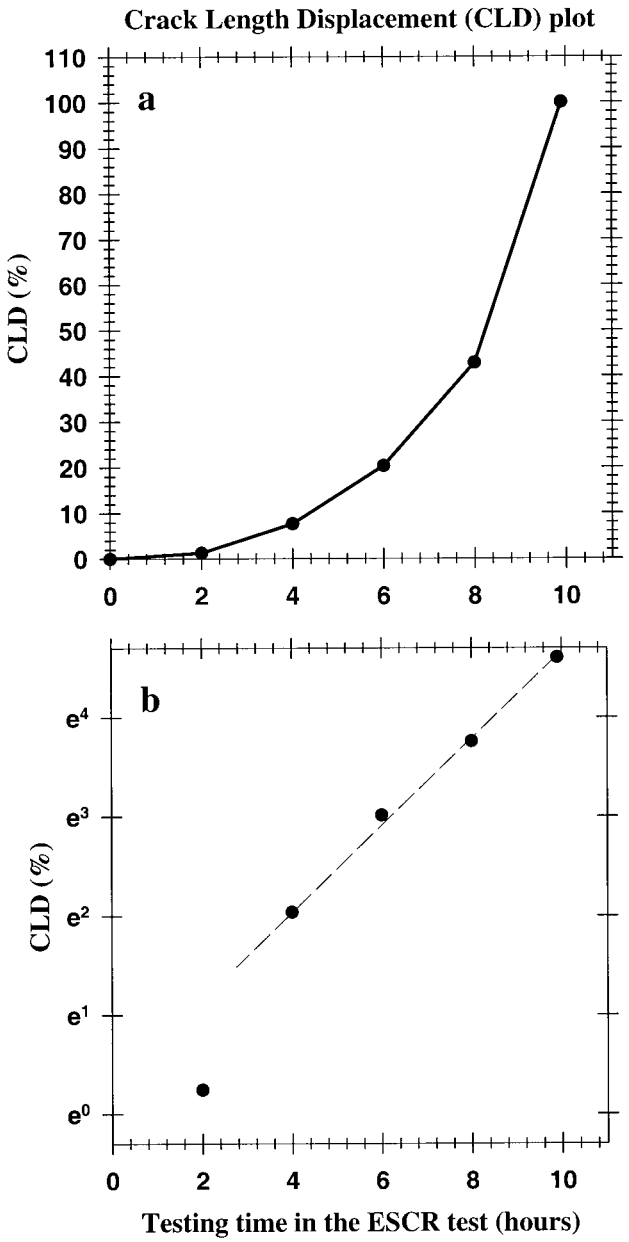

Figure 4 (a) Percent crack linear displacement (CLD) (averaged for the two notch corners of each sample and for the two samples taken out at each time interval) versus ESCR testing-time (h) on the sample CPE1. (b) CLD in a natural logarithm scale versus ESCR testing time (h); the dashed line has a slope of about 0.43.

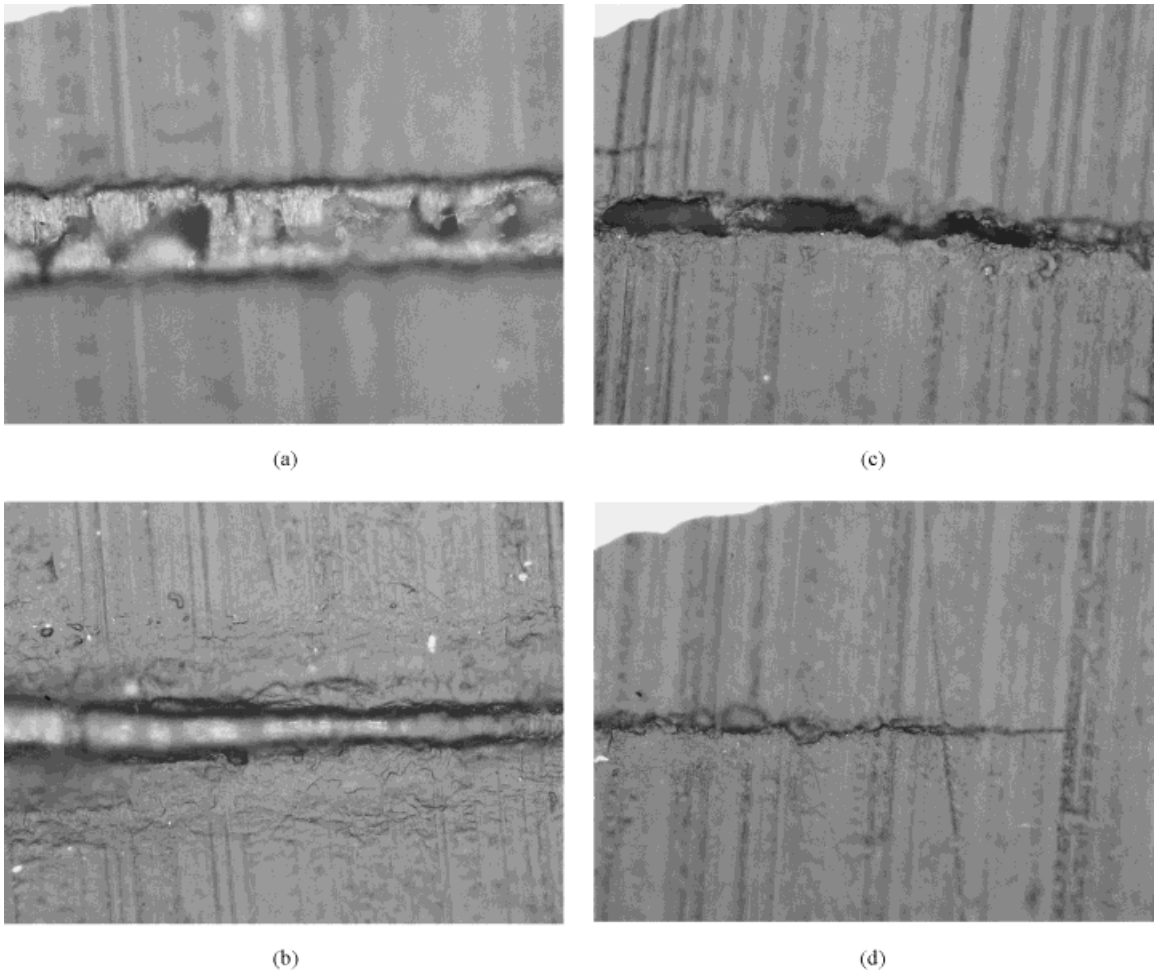

Figure 5 Optical microscopy micrographs at 60% of the failure time in the ESCR of the notch cracks and craze tips of the samples (a,b) HPE1and (c,d) HPE2. All the photographs are magnified 500×.

ure 5(a), it is observed that fibrils break down rather occur at the middle part of the fibrils (midrib). This observation is relevant to the discussion of whether fibril creep or surface drawing may be the failure mechanism applying for this sample HP1. As opposed to glassy polymers where the fibril failure is observed at the craze–bulk interface, thus supporting surface drawing, the experiments here support fibril creep. Later in the article, Raman will prove a high molecular orientation for the fibrils seen in Figure 5(a), therefore further supporting the fibril creep mechanism.

Micro-Raman Spectroscopy Study of ESCR Samples

Raman spectroscopy is sensitive to molecular orientation when adequate conditions of polarization on adequate vibrational bands are used. In PE, it is found that the intensity ratio of the 1130-cm^{-1} Raman band (assigned to the symmetrical C—C backbone vibrations) and the 1060-cm^{-1} Raman band (assigned to the asymmetrical C—C backbone vibrations) decreases with increasing molecular orientation, in the case when the direction of the molecular orientation and the laser beam polarization direction are parallel to the stress direction. (These polarization conditions will, from now on, be referred to as ″I〃 and assuming fiber-symmetric molecular orientation.[22,28–30] The deformation of PE up to the NDR results in a structure with a high orientation of the polymer chains along the strain direction. Consequently, the Raman spectra from this material will be strongly sensitive to the polarization direction of the laser and collected scattered light (see Fig. 6). As a result of this, it is possible to

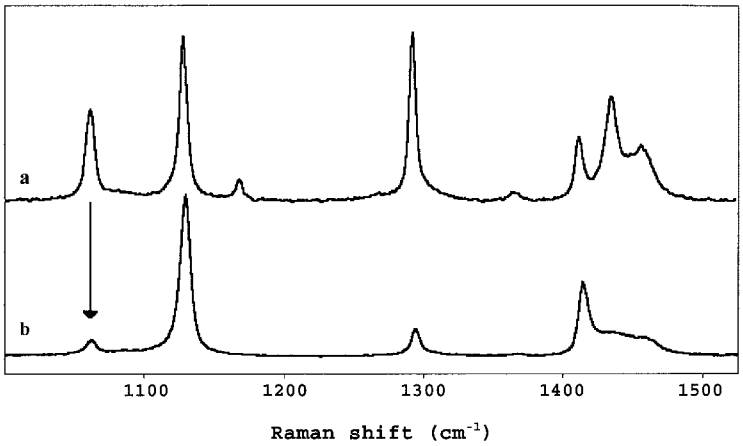

Figure 6 Polarized ″I〃 Raman spectra taken in the (a) undeformed (random orientation) material and (b) necked material (highly oriented) of sample CPE1. To record the Raman spectra, the J-Y system equipped with 600-g/mm gratings was used.

obtain an indication of the degree of the molecular orientation by measuring the relative peak areas of the backbone vibrational bands at 1130 and 1060 cm^{-1} (symmetric and asymmetric C—C stretching bands, respectively) in the spectra recorded with the ″I〃 polarization conditions. It was been proposed by Rose et al.[14] that the molecular orientation of the craze fibrils plays an important role in the ESC. Figure 7 illustrates very clearly the presence of oriented material in the crazes of the ESCR-tested samples.

From polarized Raman spectra recorded for unbroken craze fibrils of length much larger than 1 μm (lateral size of the laser spot), information concerning the molecular orientation can be calculated. In Figure 8, the area ratios of the 1130- and 1060-cm^{-1} bands taken at five different positions along the craze at different times are shown. Figure 8, therefore, presents the profile of the molecular orientation in the fibril midrib along the craze. For the 2-h sample, a flat profile indicates the absence of detectable molecular orientation. For the 8-h sample, a relatively high molecular orientation is observed. For the fibrils after 4- and 6-h testing, an increase in molecular orientation is seen. For each sample, the highest molecular orientation appears in fibrils at the crack tip. The molecular orientation diminishes toward the craze tip. In the 2- and 4-h samples, fewer and smaller fibrils are observed.

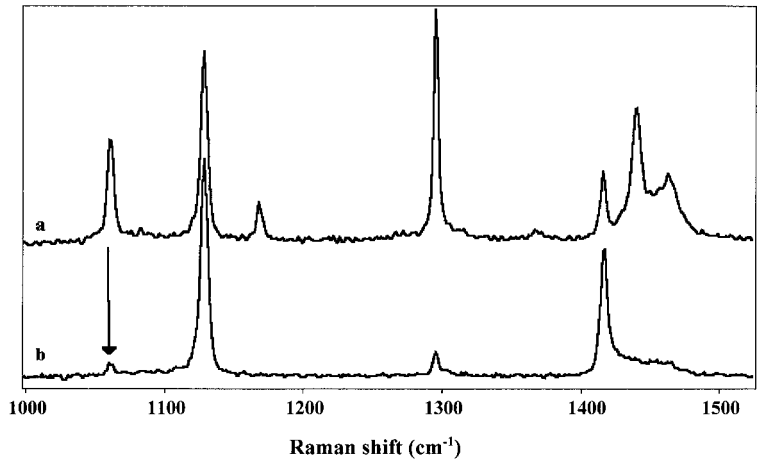

Figure 7 Polarized ″I〃 Raman spectra taken in the sample CPE1 after 9.9 h (failure time) in the ESCR test (a) outside the crack and (b) in a failed bunch of fibrils. To record the Raman spectra, the LabRam system was used. Note the similarities with Figure 6.

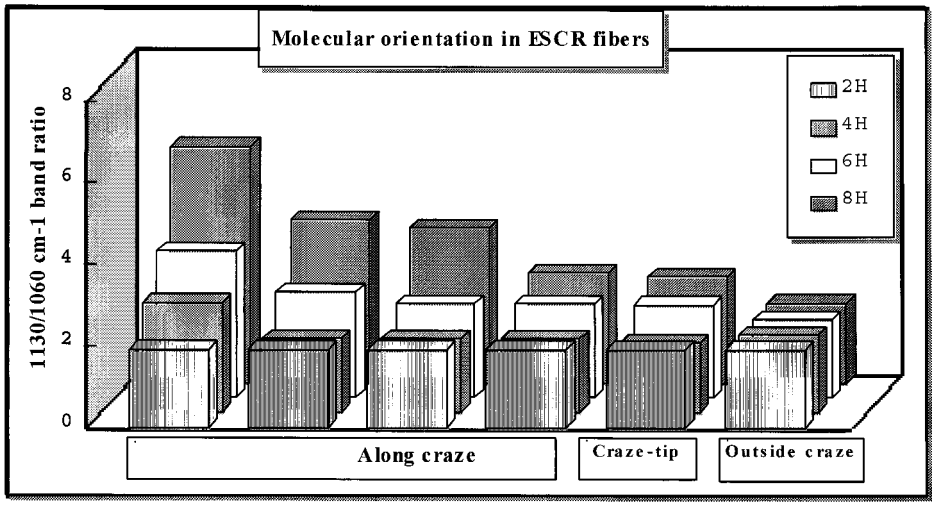

Figure 8 The 1130/1060-cm^{-1} band ratio (gives an estimation of the molecular orientation) as a function of the ESCR testing time on fibrillar material spanning the craze of sample CPE1. The J-Y system equipped with 1800-g/mm gratings was used under ″I„ polarization conditions.

This small size of the scarce fibrils at the early stages makes it difficult to focus onto the smallest fibrils, and in some cases, even at low laser powers, the thin fibrils were damaged. Therefore, the measurements at the early stages were performed mainly at the larger whitened areas (larger fibrils) seen spanning the craze. It should be remarked, however, that the laser was always focused within the craze (with thickness much greater than the lateral resolution of the Raman measurements) throughout the described experiments, and, therefore, no partial information coming from the surrounding undeformed areas (bulk) outside the craze was collected.

As a limitation of the used method, it should be noted that the spectra were recorded upon a limited number of fibrils inside the craze and in one point outside of the craze tip. For each sample, spectra in five fibrils were recorded, the fibrils being distributed over the craze. But, also, for each sample, different positions were chosen because of the dynamics of the crack opening, that is, larger crack size with increasing testing time. Spectra were recorded at the most suitable position inside the fibril. Therefore, the recorded spectra were not always taken from the exact middle of the fibril. Another source of uncertainty in the data arises from the fitting routine procedure used to determine band areas of the individual bands in the region of interest. To check the reliability, measurements were performed by several combinations of fitting conditions, that is, either fitting the 1060 and 1130 cm^{-1} with two profiles each or fitting them with only one profile each. Although differences in absolute band intensity were found, the relative band area ratio of the 1130 and 1060 cm^{-1} only slightly varied due to the fitting conditions (<5%). Finally, note that, in contrast to the previous methods used for assessing the fibril draw ratio and resulting in an average measurement throughout the fibril length,[15] here we focused the laser spot in the midrib of the fibrils. Moreover, the optical volume analyzed (laser spot size) is always constant, while the fibril size varied along the craze and crack.

In a subsequent step, Raman spectra were recorded of fibrillar material that already failed during the ESCR test (see Fig. 9). The fitting process involved only one peak per Raman band. The 1130/1060 cm^{-1} band area ratios from Figure 9 are shown in Table II. As illustrated in Figure 9 and Table II, the degree of orientation as determined from the 1130/1060-cm^{-1} band area ratio generally increases with increasing test time. The failed fibrils in the 4- and 6-h samples showed comparable molecular orientation. A remark should be made about the absolute values of the 1130/1060-band area ratios, comparing Figure 8 (data from spectra recorded with J-Y 1800 gratings) and Table II (data from spectra recorded with J-Y 600 gratings). Due to the use of the different gratings and different spectrometers, these values cannot be compared because the band profile is different (see Fig. 10).

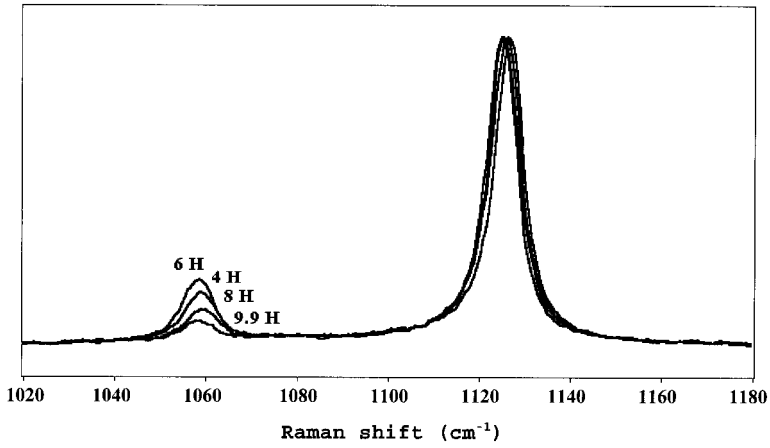

Figure 9 Raman spectra in failed fibrils taken at some time intervals of testing in the ESCR test and normalized to the 1130-cm^{-1} band on sample CPE1. The J-Y system equipped with 600-g/mm gratings was used under ″I„ polarization conditions. The spectrum at 9.9 h corresponds to the spectrum taken in the fibrillar tail of one of the two pieces left at the failure time.

Comparable experiments were performed using the Dilor Micro-Raman system with a ×100 objective and a 100-μm pinhole, resulting in higher spatial resolution (1 μm lateral, <2 μm in depth). Basically, the same results were found using this system (see Fig. 11). For the 2-h sample, the Raman spectra did not show indications of molecular orientation along the crack. For the 4-h sample, some indication of molecular orientation was found in isolated broken and in intact fibrils. For the 6- and 8-h samples, once the plastic deformation took place as the dominant crack opening mode, the presence of highly oriented material is clear. It is therefore further confirmed that the molecular orientation detected in the craze during the early hours does not seem to be as high as that detected later in the test.

Significant differences were found between HPE1 and HPE2, which are in line with the optical microscopy results (see Fig. 12). The fibrillar material in HPE1 showed a high degree of orientation. Also, in the craze tip, a high orientation was found. For HPE2, no detectable orientation was observed along the crack as is shown in Figure 12(b). A comparative summary of the observations for those low and high molecular weight homopolymers is shown in Table III.

In an additional experiment, spectra were recorded along the fibrillar axis. Thus, a single craze fibril of HPE1 removed from the test after 60% of its failure time was chosen and measured at different points along its length (see Fig. 13). Clearly, the molecular orientation is highest in the middle of the fibril (midrib area). Differences

Table II 1130/1060-cm^{-1} Band Area Ratio (Molecular Orientation) for the Cold-drawn, Creep-tested Cold-drawn Samples, and Failed Fibrils in the ESCR Test at Different Time Intervals (4, 6, 8, 9.9 h) Calculated from Polarized (″I„) Spectra Taken on Sample CPE1

Band Area Ratio	Cold-drawn CPE1	Creep-tested CPE1	Failed Fibrils in the ESCR Test (for CPE1)	
$I_{(1130/1060)}$ Voigt profiles linear baseline	20	23.1	4 h	6.3
			6 h	6
			8 h	11.8
			9.9 h (Failure)	19.14

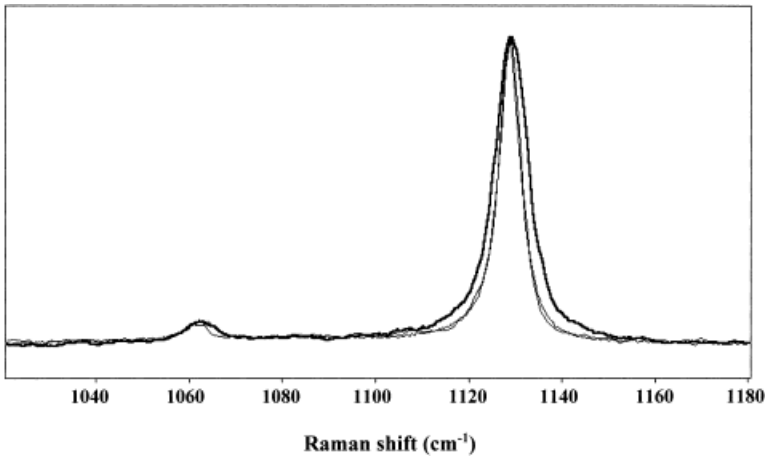

Figure 10 Polarized ″I„ Raman spectra taken in failed fibrillar material at the failure time. The spectra were recorded at about the same position with the two Raman systems using different instrumental conditions and normalized to the intensity of the 1130-cm^{-1} band. The thicker spectrum (giving a broader 1130-cm^{-1} band) was recorded with the J-Y system equipped with 600-g/mm gratings. The spectrum with smallest 1060-cm^{-1} band was recorded with the LabRam system. The third one was recorded with the J-Y system equipped with 1800-g/mm gratings.

in the degree of molecular orientation along the fibrils are expected as a consequence of the spread of draw ratios. This observation indicates that longer fibrils (crack tip fibrils) will tend to show higher molecular orientation (see Figs. 7 and 8) than that of the shorter fibrils because the constant size of the laser spot measures material with higher draw ratios. Shorter fibrils near the craze tip, on the other hand, are more likely to show a lower averaged molecular orientation.

From the previous observations, it appears that the ductile fibrils enlarge by continuous

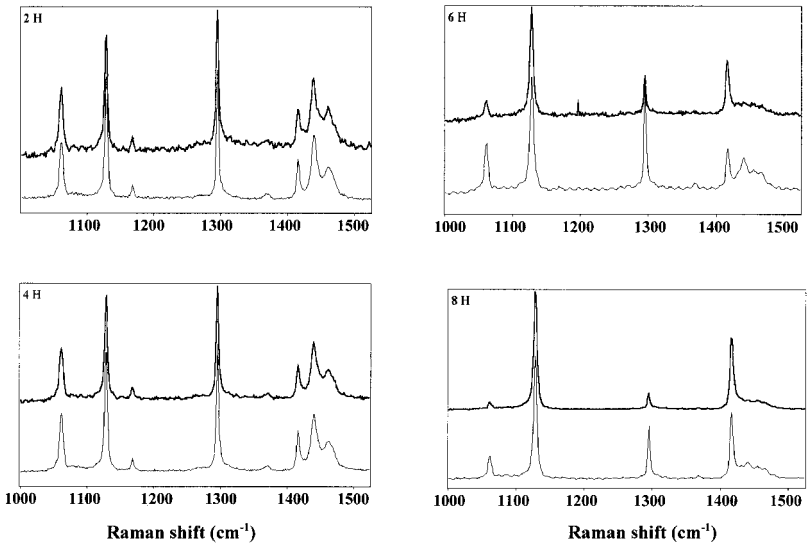

Figure 11 Polarized ″I„ Raman spectra taken in the crazes of the different samples of sample CPE1 using the LabRam system (×100 objective and 100-μm pinhole). The top spectra (thicker, shifted in the *y*-axis direction for clarity) were recorded on stress-whitened (2- and 4-h samples) material or in fibrillar material (6- and 8-h samples) spanning the crazes, and the bottom spectra were recorded at the craze tip.

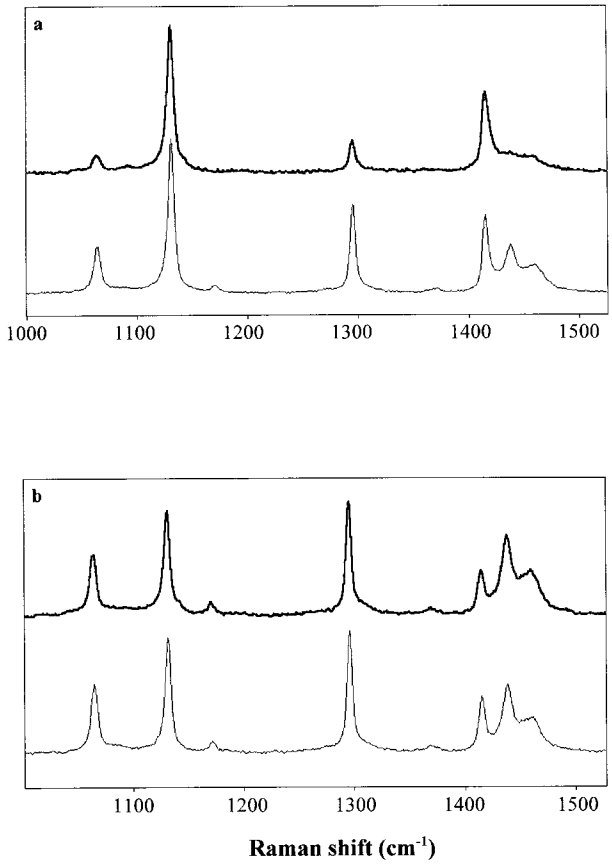

Figure 12 Polarized (I) Raman spectra taken in samples HPE1 and HPE2 at 60% of total failure in the ESCR test. The J-Y system equipped with the 600-g/mm gratings was used. (a) The top spectrum (thicker) corresponds to fibrillar material seen in Figure 5a whereas the bottom spectrum corresponds to material at the craze tip seen in Figure 5b. (b) The top spectrum (thicker) corresponds to material spanning the craze seen in Figure 5c whereas the bottom spectrum corresponds to material at the craze tip seen in Figure 5d.

drawing, and when the midrib eventually reaches a limiting draw ratio, fibril breakdown occurs via failure by creep, that is, pulling of molecules through the crystalline lamellae and molecular disentanglement in the amorphous regions.

It is of interest to monitor potential molecular stress felt by molecules in fibrils spanning the craze. When stress is applied to a polymer sample, frequency shifts, intensity, and band-shape changes are to be expected on some specific vibrational bands.[24–27] Those effects are especially evident on Raman bands with a high contribution of skeletal vibrations. In PE, the most sensitive band for monitoring the molecular strain is found to be the C—C asymmetric stretching Raman band (1060 cm^{-1}). Accordingly, we expect a small shift of this band in case the molecules within the craze fibrils are still under stress. In all craze fibrils examined, no band shifts were observed. We therefore conclude that once the applied stress (during the ESCR test) is removed, within the experimental error, no measurable residual stress is present in the structure.

Micro-Raman Spectroscopy Study of Cold-drawn and Creep-tested Samples

The spectra of the sample CPE1 cold-drawn up to the natural draw ratio and after the creep test were recorded (600-g/mm gratings) and compared to the spectra of craze fibrils. Polarized micro-Raman spectroscopy experiments were carried out on sample CPE1. As can be seen in Figure 14, the presence of highly oriented material is evident in all types of samples. The spectra recorded for the sample after the creep test presented a higher molecular orientation (the 1130/1060-cm^{-1} ratio is higher) than that of the material after just cold-drawing [see Fig. 14(a)]. The molecular orientation (expressed by the 1130/1060-cm^{-1} band area ratio, calculated after fitting the $I_{\parallel}$ spectra) for the above samples and for failed fibrils after different time-intervals (4, 6, 8, 9.9 h) in the ESCR test is shown in Table II.

From Table II, it can be seen that the molecular orientation in the failed fibrils after prolonged testing is comparable to the molecular orientation in the cold-drawn material and creep-tested materials. Finally, by considering the —CH_2— bending range at 1400–1460 cm^{-1}, and, in particular, the 1416-cm^{-1} band, differences in the relative band intensities are observed, as can be seen in Figure 14. The spectra are normalized to the intensity of the 1130-cm^{-1} band. In this case, the 1416-cm^{-1} band generally presents a higher intensity in the spectra of the ESCR samples than in the spectra of the drawn samples. The latter effect is believed to arise from differences in orthorhombic crystallinity between the samples as a consequence of the differences in the mechanical testing temperature (room temperature versus 348 K, respectively). A separate article will deal with this effect.[31]

CONCLUSIONS

Mechanical testing combined with microscopy and Raman measurements suggest the presence

Table III Correlation Table Between Results (at 60% Failure Time in the ESCR Test), Sample Characteristics, and ESCR for Samples HPE1 and HPE2

HPE2	ESCR	HPE1
Slow crack growth		Fast crack growth
High ESC resistance		Low ESC resistance
	Micro-Raman Experiments Under Polarization	
Raman spectrum of isotropiclike PE		Large ratio I_{1130}/I_{1060} Raman bands
	Molecular Deformation	
Low degree of orientation at the crack		High degree of orientation at the crack
Small plastic deformation		Large scale plastic deformation
Brittle behavior		Ductile behavior
	Sample Characteristics	
(HDPE) High molecular weight		(HDPE) Low molecular weight
Low density		High density
Low NDR		High NDR
	Optical Microscopy	
Sharp craze tip		White and blunt craze tip
Poor fibrillar formation, small size fibril		Extensive fibrillar formation, large size fibril
Small crack opening		Large crack opening

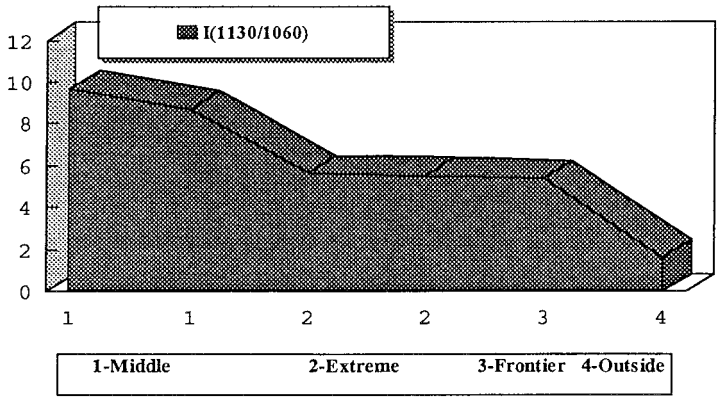

Figure 13 Profile of molecular orientation (1130/1060 cm^{-1}) along a fibril spanning the craze of a sample taken out of the ESCR test at 60% of the failure time (on sample HPE1). Six spectra were taken along the fibril. "Outside" means at the craze side, "frontier" means at the craze surface where the fibrillar bunch dies, "extreme" means at the closest parts of the fibril to the craze surface, and "middle" means at the middle part of the fibril.

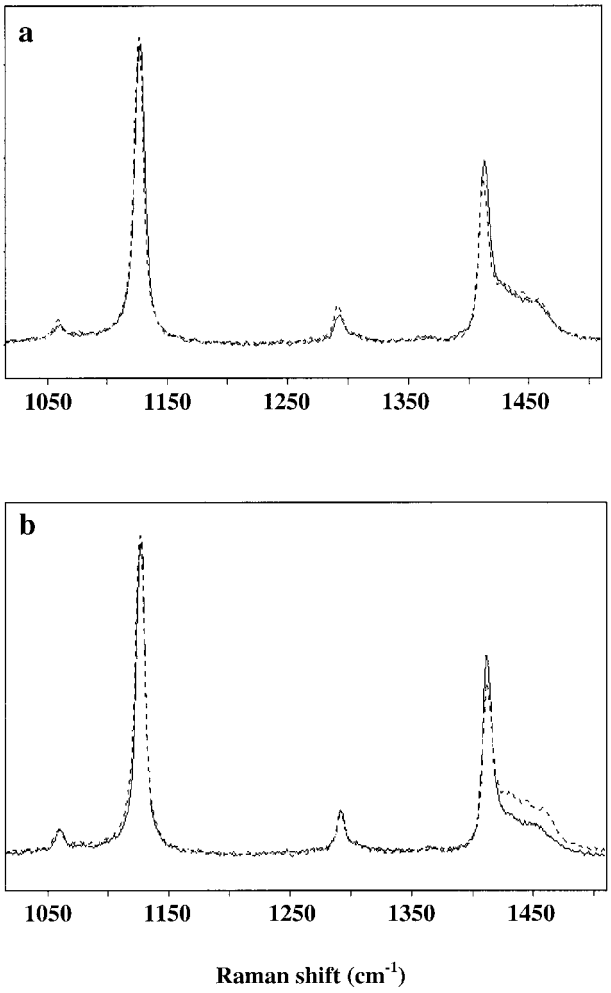

Figure 14 Polarized $''I_v$ Raman spectra taken on sample CPE1: (a) (dashed) spectra taken in cold-drawn material and in creep tested cold-drawn material; (b) (dashed) spectrum taken in cold-drawn material and in failed fibrillar material in the 9.9-h sample.

of two distinct failure regimes in the ESCR experiments. In the early stages of crack development, that is, for times <40% of the failure time in sample CPE1, limited fibrillation occurs and brittle failure is observed. The failure pattern is typical for PE at low stress. The observation of low deformation at the crack tip during the brittle stage was already recognized by Lustiger et al.[13] Those authors proposed that the uniform deformation of the fibrils is considerably interrupted by "interlamellar failure" produced by either the disentangling or rupture of tie molecules. This contrasts sharply with the behavior observed at larger times, that is, larger than 40% of the failure time. Here, crack growth accelerates steadily with an exponential profile. The process is associated with extensive ductility, that is, formation of highly drawn fibrils. Clearly, it is this stage of the process that has particular relevance to the ultimate failure of the ESCR sample. Moreover, it is apparent that distinct and perhaps more complex fracture morphology is observed in PE when compared to glassy polymers.

The micro-Raman technique used in this study is a powerful means to probe the molecular orientation in both cases. It has been found that the level of orientation in the ductil fibrils of the ESCR samples is comparable to that of samples drawn to their natural draw ratio and decreases from crack to craze tip. This evidence fully supports the model by Rose et al.[14] which associates ESCR failure time to the rupture performance of the craze fibrils. Moreover, the choice of drawn specimens to mimic the behavior of such fibrils appears justified.

The present work also suggests that the extent, over the testing time, of the brittle stage of failure, showing scarce fibrillar formation, small fibril size, and lack of detectable craze molecular orientation, is dependent upon the polymer molecular weight. Thus, the brittle stage of failure seems to last longer in samples with high molecular weight. This picture is in accordance with a recent work,[27] which showed that the molecular stress is lower at high molecular weights, therefore maintaining the craze in a low local stress regime brittlelike for longer. Consistently with previous work,[32] the maximum draw ratio attained decreases with increasing molecular weight.

The authors are grateful to DSM Research and BP Chemicals for granting permission to publish this work.

REFERENCES

1. Brown, N.; Bhatacharya, S. K. Mater Sci 1985, 20, 4553.
2. Lu, X.; Brown, N. Polymer 1987, 28, 1505.
3. Wang, X.; Brown, N. Polymer 1988, 29, 463.
4. Lu, X.; Wang, X.; Brown, N. J Mater Sci 1988, 23, 643.
5. Wang, X.; Brown, N. Polymer 1989, 30, 1456.
6. Ward, A. L.; Lu, X.; Brown, N. Polym Eng Sci 1990, 30, 1175.
7. Huang, Y. L.; Brown, N. J Polym Sci Part B Polym Phys 1990, 28, 2007.
8. Huang, Y. L.; Brown, N. J. Polym Sci Part B Polym Phys 1991, 29, 129.

9. Brown, N.; Lu, X.; Huang, Y. L.; Qian, R. Makromol Chem Macromol Symp 1991, 41, 55.
10. Barry, D.; Delatycki, O. J Polym Sci Part B Polym Phys 1987, 25, 883.
11. Barry, D.; Delatycki, O. Polymer 1992, 33, 1261.
12. Brown, N;. Lu, X.; Huang, Y.-L.; Qian, R. Makromol Chem Macromol Symp 1991, 41, 55.
13. Lustiger, A.; Corneliusen, R. D. J Mater Sci 1987, 22, 2470.
14. Rose, L. J.; Channel, A. D.; Frey, C. J.; Gapaccio, G. J Appl Polym Sci 1994, 54, 2119.
15. Kramer , E. J. in "Plastic deformation of amorphous and semi-crystalline materials," eds. B. Escaig and C. H. G'sell. Editions de Physique EPD Sciences Editorial, Les Houches (1982), pg 391. Hui, C. Y.; Ruina, A.; Creton, C.; Kramer, E. J. Macromolecules 1992, 25, 3948.
16. Kausch, H. H. Crazing in Polymers; Springer-Verlag: Berlin, 1990; Vol. 2.
17. Meier, R. J.; Kip, B. J. Microbeam Anal 1994, 3, 61.
18. Tabaksblat, R.; Meier, R. J.; Kip, B. J Appl Spectrosc 1992, 46, 60.
19. Markwort, L.; Kip, B.; Da Silva, E.; Roussel, B. Appl Spectrosc 1995, 49, 1411.
20. Schachtschneider, J. H.; Snyder, R. G. Spectrochim Acta 1963, 19, 117.
21. Strobl, G. R.; Hagedorn, W. J Polym Sci Polym Phys Ed 1978, 16, 1181.
22. Pigeon, M.; Prud′homme, R. E.; Pezolet, M. Macromolecules 1991, 24, 5687.
23. Gordeyev, S. A.; Nikolaeva, G. Yu.; Prokhorov, K. A. Laser Phys 1996, 6, 121.
24. Kip, B. J.; van Eijk, M. C. P.; Meier, R. J. J Polym Sci Polym Phys 1991, 29, 99.
25. Moonen, J. A. H. M.; Roovers, W. A. C.; Meier, R. J.; Kip, B. J. J Polym Sci Polym Phys 1992, 30, 361.
26. Rodriguez-Cabello, J. C.; Merino, J. C.; Jawhari, T.; Pastor, J. M. Polymer 1995, 36, 4233.
27. Lagaron, J. M; Dixon, N. M.; Reed, W.; Gerrard, D. L.; Kip, B. J. Macromolecules 1998, 31, 5845.
28. Masetti, G.; Abbate, S.; Gussoni, M.; Zerbi, G. J Chem Phys 1980, 73, 4671.
29. Kip, B. J.; van Gurp, M.; van Heel, S. P. C.; Meier, R. J. J Raman Spectrosc 1993, 24, 501.
30. Citra, M. J.; Chase, D. B.; Ikeda, R. M.; Gardner, K. H. Macromolecules 1995, 28, 4007.
31. Lagaron, J. M.; Dixon, N. M.; Reed, W.; Pastor, J. M.; Kip, B. K. Polymer 1999, 40, 2569.
32. Capaccio, G.; Crompton, T. A.; Ward, I. M. J Polym Sci Phys 1976, 14, 1641.